Monthly Notices
of the
ROYAL ASTRONOMICAL SOCIETY

MNRAS **513,** 4037–4044 (2022)
Advance Access publication 2022 April 27

https://doi.org/10.1093/mnras/stac1082

Detection of quasi-periodic micro-structure in three millisecond pulsars with the Large European Array for Pulsars

K. Liu,[1★] J. Antoniadis,[1,2,3] C. G. Bassa,[4] S. Chen,[5,6] I. Cognard,[5,6] M. Gaikwad,[1] H. Hu,[1] J. Jang,[1] G. H. Janssen,[4,7] R. Karuppusamy,[1] M. Kramer,[1,8] K. J. Lee,[9] R. A. Main,[1] G. Mall,[1,10,11] J. W. McKee,[10] M. B. Mickaliger,[8] D. Perrodin,[12] S. A. Sanidas,[8] B. W. Stappers,[8] L. Wang,[8,13] W. W. Zhu,[13] M. Burgay,[12] R. Concu,[12] A. Corongiu,[12] A. Melis,[12] M. Pilia[12] and A. Possenti[12,14]

[1] *Max-Planck-Institut für Radioastronomie, Auf dem Hügel 69, D-53121 Bonn, Germany*
[2] *Institute of Astrophysics, FORTH, Department of Physics, University of Crete, Voutes, University Campus, GR-71003 Heraklion, Greece*
[3] *Argelander Institut für Astronomie, Auf dem Hügel 71, D-53121 Bonn, Germany*
[4] *ASTRON, the Netherlands Institute for Radio Astronomy, Oude Hoogeveensedijk 4, NL-7991 PD Dwingeloo, the Netherlands*
[5] *Laboratoire de Physique et Chimie de l'Environnement et de l'Espace LPC2E CNRS-Université d'Orléans, F-45071 Orléans, France*
[6] *Station de radioastronomie de Nançay, Observatoire de Paris, PSL Research University, CNRS/INSU F-18330 Nançay, France*
[7] *Department of Astrophysics/IMAPP, Radboud University, PO Box 9010, NL-6500 GL Nijmegen, the Netherlands*
[8] *Jodrell Bank Centre for Astrophysics, School of Physics and Astronomy, The University of Manchester, Manchester M13 9PL, UK*
[9] *Kavli institute for astronomy and astrophysics, Peking University, Beijing 100871, P. R. China*
[10] *Canadian Institute for Theoretical Astrophysics, University of Toronto, 60 St George Street, Toronto, ON M5S 3H8, Canada*
[11] *Department of Physics, University of Toronto, 60 St. George Street, Toronto, ON M5S 1A7, Canada*
[12] *INAF - Osservatorio Astronomico di Cagliari, via della Scienza 5, I-09047 Selargius (CA), Italy*
[13] *National Astronomical Observatories, Chinese Academy of Sciences, A20 Datun Rd, Chaoyang District, Beijing 100012, P. R. China*
[14] *Dipartimento di Fisica, Università di Cagliari, S.P. Monserrato-Sestu Km 0,700, I-09042 Monserrato (CA), Italy*

Accepted 2022 April 13. Received 2022 April 11; in original form 2022 January 6

ABSTRACT

We report on the detection of quasi-periodic micro-structure in three millisecond pulsars (MSPs), PSRs J1022+1001, J2145−0750, and J1744−1134, using high time resolution data acquired with the Large European Array for Pulsars at a radio frequency of 1.4 GHz. The occurrence rate of quasi-periodic micro-structure is consistent among pulses with different peak flux densities. Using an auto-correlation analysis, we measure the periodicity and width of the micro-structure in these three pulsars. The detected micro-structure from PSRs J1022+1001 and J1744−1134 is often highly linearly polarized. In PSR J1022+1001, the linear polarization position angles of micro-structure pulses are in general flat with a small degree of variation. Using these results, we further examine the frequency and rotational period dependency of micro-structure properties established in previous work, along with the angular beaming and temporal modulation models that explain the appearance of micro-structure. We also discuss a possible link of micro-structure to the properties of some of the recently discovered fast radio bursts which exhibit a very similar emission morphology.

Key words: methods: data analysis – pulsars: individual (PSR J1022+1001) – pulsars: individual (PSR J2145−0750) – pulsars: individual (PSR J1744−1134) – (transients:) fast radio bursts.

1 INTRODUCTION

Pulsars exhibit a large variety of radio emission phenomena on a wide range of time-scales, which is still to be fully understood. The very first pulsar observations already revealed the significant variability among the pulses from every rotational period. In particular, some pulses show concentrated emission in sub-millisecond features, usually with a typical width and sometimes a quasi-periodicity (Craft, Comella & Drake 1968; Hankins 1972). These so-called *micro-structure* phenomena have been seen in a number of canonical pulsars (e.g. Cordes, Weisberg & Hankins 1990; Lange et al. 1998; Kramer, Johnston & van Straten 2002), and recently also in millisecond pulsars (MSPs; De, Gupta & Sharma 2016). Many of the micro-structure pulses exhibit significant fraction of polarization (e.g. Mitra, Arjunwadkar & Rankin 2015; De et al. 2016), higher than those expected from the average pulse profile. Simultaneous observations at multiple frequencies have shown that micro-structures occur over a wide frequency range at the same time (e.g. Rickett, Hankins & Cordes 1975; Boriakoff, Ferguson & Slater 1981), which suggests a fundamental association of micro-structure with the pulsar emission process.

So far, a number of models have been developed to explain the appearance of micro-structure in pulsars. Generally, these models can be categorized into two types of scenarios. The first one involves an angular radiation pattern as a result of multiple thin flux tubes along

---

★ E-mail: kliu.psr@gmail.com

the magnetic field lines where streaming bunches of charged particles radiate in the direction of propagation (e.g. Benford 1977). As the pulsar rotates, the emission structure is then sampled in time. The width of the micro-structure, in this case, would correspond to the angular beamwidth of the radiation. The second scenario includes a temporal intensity modulation of the emission, and may be caused by electrodynamical fluctuations (Buschauer & Benford 1980; Cheng & Ruderman 1980), neutron star vibrations (Van Horn 1980; Clemens & Rosen 2004), or radiation transfer effects (Harding & Tademaru 1981; Cairns, Johnston & Das 2004). Here, the micro-structure width reflects the actual time-scale of the emission, which may be related to the radial structure in the plasma outflow.

Most of micro-structure studies focus on measuring their temporal width and quasi-periodicity, and relating them with other properties such as pulsar rotational period and observing frequency (e.g. Cordes 1979; Kramer et al. 2002; Mitra et al. 2015). These help to distinguish between the two possible scenarios for micro-structure, possibly identifying the physical mechanism of the emission. To date, the majority of micro-structure investigations have been based on canonical pulsars. Extending the analysis to MSPs would allow to examine the existing theories in a broader parameter (e.g. the pulsar period) space and with new samples. Comparing the results obtained from canonical pulsars and MSPs would also reveal whether micro-structure is a common feature for all pulsar populations.

Finding micro-structure emission in MSPs is in general difficult mainly due to the limitation of sensitivity and other technical constraints such as time and frequency resolution of the recorded data. As a result, the first micro-structure detection in MSPs has only been achieved recently (De et al. 2016), following a small number of reported non-detections (Jenet et al. 1998; Sallmen 1998; Jenet, Anderson & Prince 2001; Liu et al. 2016). The Large European Array for Pulsars (LEAP) is the ideal instrument to study micro-structure emission from pulsars. LEAP coherently combines pulsar observations from the five largest radio telescopes in Europe: the 100-m Effelsberg Telescope in Germany, the 76-m Lovell Telescope at Jodrell Bank Observatory (JBO) in the UK, the 94-m equivalent Nançay Radio Telescope in France, the 64-m Sardinia Radio Telescope in Italy, and the 94-m equivalent Westerbork Synthesis Telescope in the Netherlands. This delivers a sensitivity equivalent to a 194-m single dish (Bassa et al. 2016). The boost in sensitivity is not only important for high-precision pulsar timing, but has also allowed for other pulsar projects that are largely limited by sensitivity with smaller telescopes, such as single-pulse and scintillation studies of MSPs (Liu et al. 2016; McKee et al. 2019; Main et al. 2020). In particular, the baseband recording and storage capability enables LEAP to generate data products with customized time and frequency resolutions and coherent de-dispersion for these studies.

The rest of the paper is organized as follows. In Section 2, we describe the observations and post-processing of the data. In Section 3, we present the detection of micro-structure in three MSPs and the measurements of their properties. Section 4 includes a brief discussion on the results and conclusions can be found in Section 5.

2 OBSERVATIONS

LEAP conducts monthly observations of over 20 MSPs at *L* band (1396 MHz), for the main purpose of detecting low-frequency gravitational waves with the PTA experiment (Chen et al. 2021). To allow studies of micro-structure in MSPs, observations where a significant number of single pulses can be clearly detected are needed. Therefore, here we selected three bright MSPs: J1022+1001, J2145−0750, J1744−1134. For each source, we selected the observation epoch when the pulsar signal was greatly amplified by interstellar scintillation, achieving the highest signal-to-noise ratio (S/N) of detection per unit time in the set of all our observations. During the observation, the astronomical signals were sampled at Nyquist rate with 8 bits and recorded on spinning discs as baseband voltages with a bandwidth of 128 MHz. The data collected at each individual telescope were later transferred to our storage server at JBO, where they were correlated, calibrated for polarization, and coherently combined using a dedicated software correlator (Smits et al. 2017). Next, the combined baseband data from those epochs were processed to produce single-pulse data (i.e. one archive per rotation) with the specifications given in Table 1. The single-pulse data were then cleaned to remove narrow-band radio interference. The rotation measure values from Dai et al. (2015) were used to correct for the Faraday rotation in the polarization. These data-processing steps used the PSRCHIVE software package (Hotan, van Straten & Manchester 2004). Fig. 1 presents the average profiles of the three pulsars each obtained from the single-epoch observation listed in Table 1. They are highly consistent with previously reported averaged profiles obtained by adding many hours of observations (e.g. Dai et al. 2015), demonstrating the high quality of the coherent combined LEAP data.

3 RESULTS

The single-pulse data were used to search for and investigate micro-structure emission from each of the selected pulsars. We first calculated the peak S/N of all single pulses and selected those with $S/N > 6$. This left 7.4, 4.2, 1.4 per cent of all recorded pulses for PSR J1022+1001, J2145−0750, J1744−1134, respectively. We then calculated the autocorrelation function (ACF) of the on-pulse region for each of the selected pulses. The presence of quasi-periodic micro-structure would manifest itself by exhibiting equally spaced maxima in the ACF, with the time lag of the first maxima corresponding to the characteristic temporal separation, i.e. periodicity of the micro-pulses (e.g. Cordes 1979; Lange et al. 1998; Kramer et al. 2002). We also generated the ACF with a linear fit (to itself) subtracted, which in some cases makes the maxima in the ACF more prominent. Next, we visually checked all the selected pulses along with their ACFs to identify those exhibiting micro-structure emission. For pulses with regularly spaced maxima in the ACF, we recorded the time lag of the first maxima as the quasi-periodicity P_μ of the micro-structure. The micro-structure width τ_μ was measured using the average ACF of all pulses with micro-structure detected, which corresponds to the first sign change in the ACF slope (see e.g. fig. 1 of Kramer et al. 2002).

3.1 J1022+1001

Approximately 37 per cent of the S/N>6 pulses that have been viewed show micro-structure emission, and 3 per cent exhibit quasi-periodicity. The top panels in Fig. 2 show two typical examples. The vast majority of these pulses coincide in phase with the trailing component of the average pulse profile (see Fig. 1). This is consistent with the findings in Liu et al. (2015) where most of the detected bright single pulses are from the trailing component as a result of its high intensity modulation (Edwards & Stappers 2003). Most micro-structure pulses are seen to have a high degree of linear polarization and some with a clear circular component, in agreement with the average polarization profile. Fig. 3 presents the distribution of the measured periodicities for those showing quasi-periodic features,

Table 1. Properties of the pulsars and details of the data investigated in this paper. Here, P, $T_{\rm int}$, Δt, $N_{\rm p}$, and $\rho_{\rm S/N>6}$ represent the pulsar rotational period, duration of the observation, time resolution of the single-pulse data, total number of pulses recorded, and the percentage of pulses with peak S/N higher than 6. The single-pulse data for each pulsar were coherently de-dispersed with the DM values given below and retain a 1-MHz frequency resolution over the 128-MHz bandwidth. The measurements of micro-structure (median) quasi-periodicity (P_μ) and width (τ_μ) are also listed.

Jname	P (ms)	DM (cm^{-3} pc)	MJD	$T_{\rm int}$ (min)	Δt (µs)	$N_{\rm p}$	$\rho_{\rm S/N>6}$	P_μ (µs)	τ_μ (µs)
J1022+1001	16.45	10.2595	56739.9	43.0	2.03	~154 500	7.4 per cent	$14.9^{+5.2}_{-2.8}$	9 ± 1
J2145−0750	16.05	8.9953	56740.4	32.0	1.96	~119 600	4.2 per cent	$17.8^{+2.7}_{-3.2}$	10 ± 1
J1744−1134	4.07	3.1380	57107.2	38.8	0.99	~567 100	1.4 per cent	$6.0^{+2.4}_{-0.8}$	3.9 ± 0.5

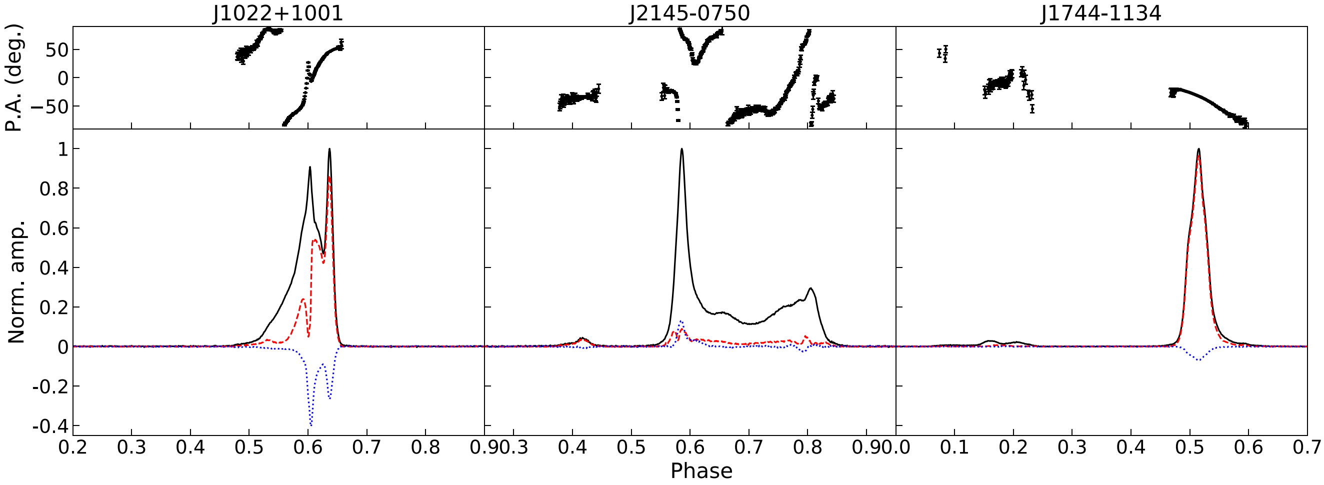

Figure 1. Polarization profiles and the linear polarization position angles (P.A.) of the three MSPs from our observations listed in Table 1. The black solid, red dashed, and blue dotted lines represent the total intensity, linear, and circular polarization, respectively.

which ranges in the 10–30 µs interval with a median P_μ of 14.9 µs. In addition to the total intensity, we also searched for quasi-periodic micro-structure in the linear and circular components of the pulses and found consistent periodicities, similar to what has been reported by Mitra et al. (2015) for canonical pulsars. Averaging the ACFs from all these pulses, we obtained a characteristic width of $\tau_\mu = 9 \pm 1$ µs. Fig. 4 shows the distribution of quasi-periodic micro-structure pulses with respect to their peak flux density relative to the average of all pulses. It can be seen that quasi-periodic micro-structure occurs in pulses of different peak flux densities, including the brightest ones. The detection rate is found to be roughly independent of the peak flux density, with a potential small preference to stronger pulsars, which however needs to be confirmed with more samples.

Fig. 5 compares the linear polarization position angles (P.A.) of the quasi-periodic micro-structure pulses with that obtained from the average profile. Here, for each individual phase bin, a probability density distribution of P.A. was formed based on the measurements from these pulses. It can be seen that on average, the P.A. swings from the micro-structure pulses and average profile are highly consistent. Still, the P.A. swing from each pulse does exhibit additional variations within a small range. This can be seen in the three examples shown in Fig. 5, which exhibit different gradients of change in pulse phase. Overall, the P.A. values of micro-structure pulses fall in a narrow range, mostly because they are obtained from a narrow window in pulse phase, which corresponds to approximately only 1.5 per cent of the entire rotational period. This is significantly narrower compared to the entire on-pulse region of the average profile, which spans 20 per cent of the spin period as shown in Fig. 1.

3.2 J2145−0750

Approximately 38 per cent of the S/N>6 pulses show micro-structure and 3 per cent exhibit quasi-periodicity. Two examples of quasi-periodic micro-structure can be found in Fig. 2. All micro-structure detections cluster around the phase of the primary component in the averaged pulse profile (see Fig. 1). The micro-structures generally are weakly polarized, which is in line with the average polarization profile shown in Fig. 1, and seemingly different from the finding at 630 MHz reported by De et al. (2016). Still, occasionally some of the micro-pulses do show a high degree of polarization which is up to ~100 per cent and can be either linear or circular. As shown in Fig. 3, the measured micro-structure periodicities range in the 10–25 µs interval with a median P_μ of 17.8 µs. From the number distribution in Fig. 4, it can be seen that the occurrence rate of micro-structure is in general uniform as a function of peak flux density, including the brightest group of pulses. The micro-structure time-scale was measured to be $\tau_\mu = 10 \pm 1$ µs from the averaged ACFs of all micro-structure pulses.

3.3 J1744−1134

About 14 per cent of the pulses that have been visually inspected show micro-structure, and 1 per cent exhibit quasi-periodic features. Two examples of the quasi-periodic micro-structure detections are found in Fig. 2. Similar to the situation in J2145−0750, all of these detections are associated with the primary component in the average profile shown in Fig. 1. As seen in Fig. 3, the measured periodicity of the micro-structures varies from 4 to 12 µs, with a median P_μ of 6.0 µs. Averaging the ACFs of all micro-structure pulses, we obtained

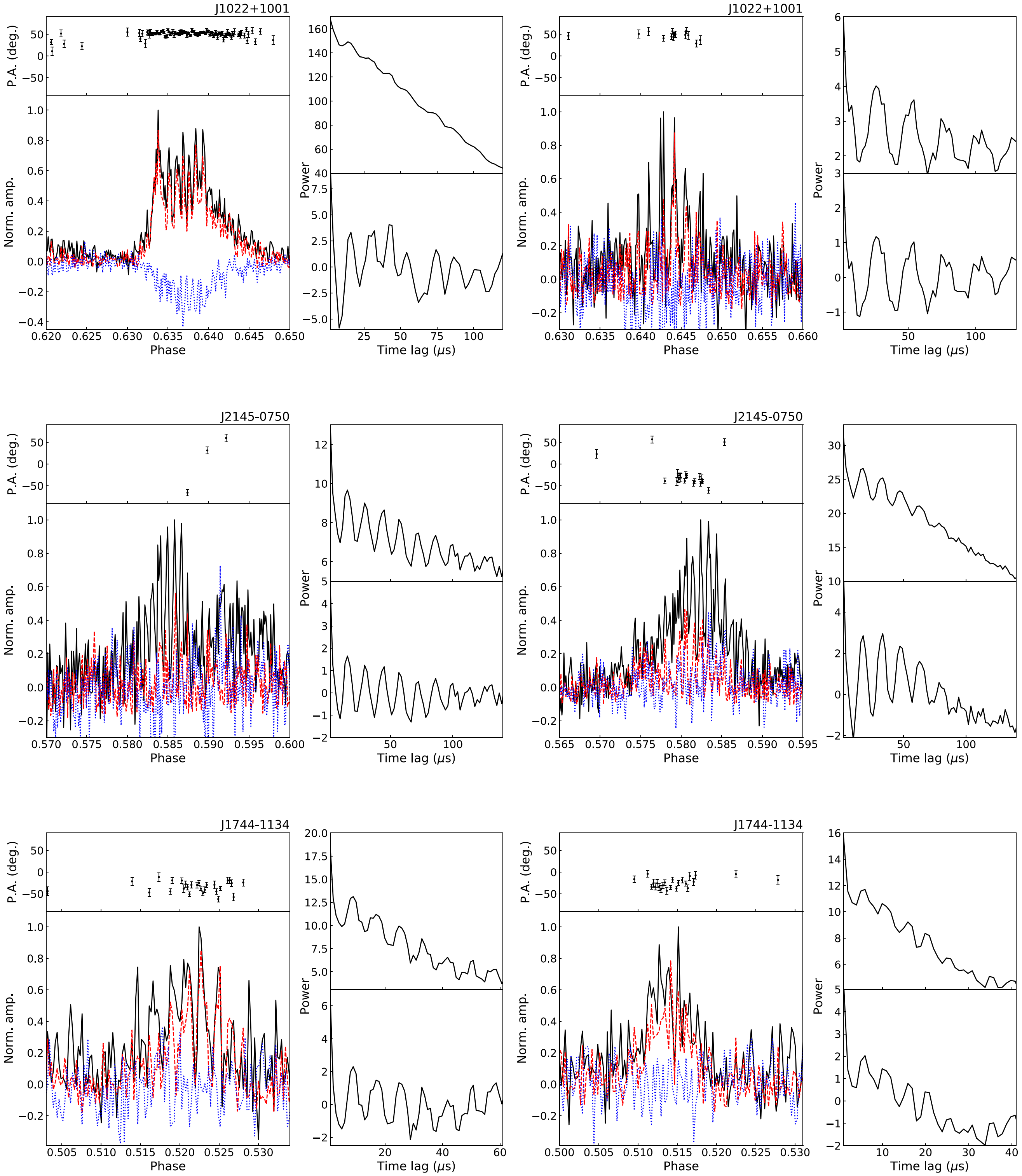

Figure 2. Examples of pulses showing quasi-periodic micro-structure from PSRs J1022+1001 (first row), J2145−0750 (second row), and J1744−1134 (third row). The first and third column of panels show the pulse intensities and their linear polarization position angles (P.A.), where the black solid, red dashed, and blue dotted lines represent total intensity, linear, and circular polarization, respectively. The second and fourth column of panels present the ACFs of the pulses shown on their left (upper), and the same ACFs but with a linear fit subtracted (lower). Note that for each pulsar, the two example pulses are aligned in phase with respect to the rotational period.

a micro-structure time-scale of $\tau_{\mu} = 3.4 \pm 0.5\,\mu\mathrm{s}$, after correcting for the sampling width. Most of the micro-structure pulses exhibit a high degree of linear polarization, in line with the feature seen in the average profile as shown in Fig. 1. The linear component also shows periodicities consistent with those from the total intensity. As shown in Fig. 4, the occurrence rate of quasi-periodic micro-structure is generally constant for pulses of different peak flux densities.

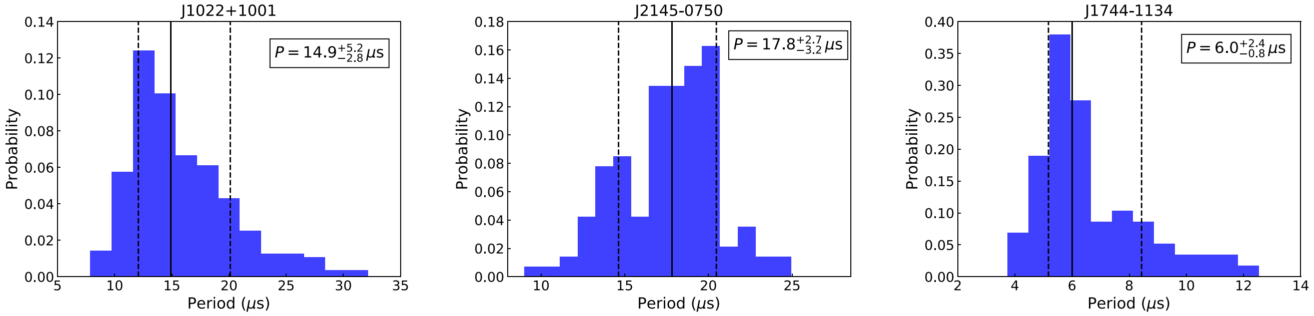

Figure 3. Histogram of micro-structure periodicity measured in J1022+1001 (left), J2145−0750 (middle), and J1744−1134 (right). In each plot, the solid line represents the median of the distribution and the two dashed lines marks the 1σ confidence interval counting from the median to both sides.

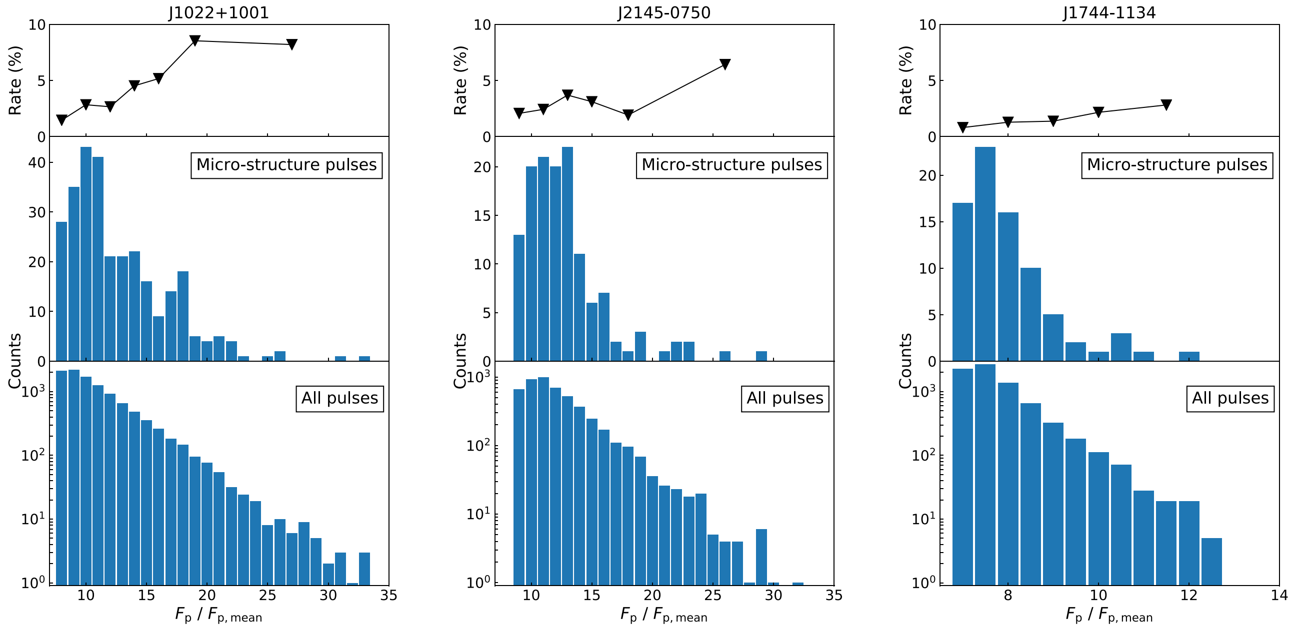

Figure 4. Distribution of normalized peak flux density (with respect to the mean of all pulses) of micro-structure pulses in comparison with that of all pulses, for J1022101 (left), J2145−0750 (middle), and J1744−1134 (right). The top panels show the percentage detection rate of quasi-periodic micro-structure pulses.

4 DISCUSSIONS

4.1 Detection rate of micro-structure

The fractions of pulses detected with quasi-periodic micro-structure are small in comparison with those reported in many canonical pulsars (e.g. Lange et al. 1998). In theory, an apparent quasi-periodicity may be produced by an uncorrelated intensity variation at different pulse phases, given that the number of samples is significant enough. To examine the potential impact of such an effect on our results, for each pulsar we randomly chose a stack of 1500 pulses and carried out the following experiment. For each individual pulse phase, we first randomly shuffled the order of intensity bins in the stack. We then calculated the ACFs of the pulses in the new stack and visually inspected the result to obtain the number of detections. This experiment has been carried out to all of the three pulsars, which gave detection rates of quasi-periodic micro-structure pulses of 0.4 per cent, 0.3 per cent, 0.1 per cent for PSRs J1022+1001, J2145−0750, J1744−1134, respectively. These are all approximately an order-of-magnitude lower than the those from the real data. This suggests that the detected quasi-periodic micro-structures in these pulsars are unlikely to be solely attributed to uncorrelated intensity variation in pulse phase.

4.2 Frequency dependency of micro-structure

The micro-structure periodicity of PSR J2145−0750 measured with our *L*-band observation is highly consistent with the value obtained at 610 MHz by De et al. (2016), suggesting that the micro-pulse separation of this pulsar is likely to be frequency independent. This is similar to what has been observed so far in many young pulsars (Cordes et al. 1990; Mitra et al. 2015), but is the first time it has been observed in an MSP. The frequency independence of micro-structure separation better supports the temporal radial origin of micro-structure scenario (Cordes et al. 1990), as in the angular beaming model, the separation is supposed to evolve as a function of observing frequency if it follows the radius-to-frequency mapping. However, we noticed that the pulse profile of J2145−0750 has a very similar width within a wide frequency range from 100 MHz to at least 5 GHz (Kramer et al. 1999). Though the profile shape of PSR J2145−0750, primarily the amplitude ratio between the

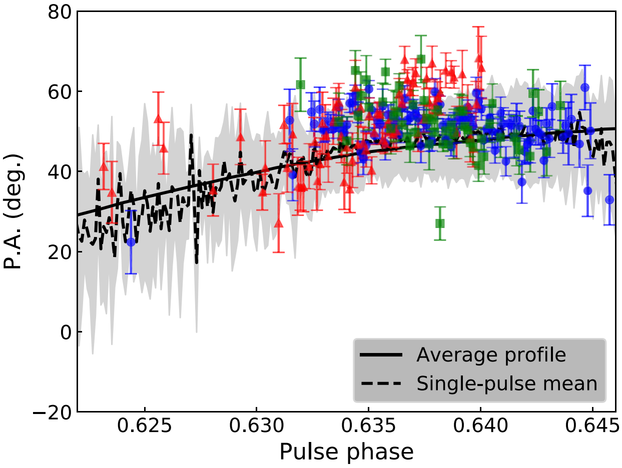

Figure 5. Comparison of P.A. swings from PSR J1022+1001. The solid black line is the P.A. swing from the integrated profile shown in Fig. 1. The dashed black line represents the weighted mean from all micro-structure pulses, while the shallow grey band represents the 1σ probability range. The red triangles, blue dots, and green squares are P.A. values from three example micro-structure pulses, respectively. The first shows a steeper increase of P.A. in pulse phase, the second is mostly steady, and the third has an opposite sign of gradient.

two main components, changes significantly in frequency, this may well be explained by the difference in spectral index of emission components as seen in other pulsars (e.g. Keith et al. 2011). Thus, these suggest that the frequency dependency of micro-structure is unlikely to be significant in J2145−0750 due to the fairly consistent emission beamwidth at multiple frequencies.

Our 3 per cent detection rate of micro-structure in J2145−0750 is a factor of a few lower than that reported by De et al. (2016). While the observing times investigated are approximately the same, De et al. (2016) reported over 700 pulses with an S/N above 15 but there are only 33 in our case. To obtain a total number of 700 pulses from our observations, the S/N threshold needs to be set at 9.3. The detection rate for this group is approximately 3.5 per cent and thus with no significant difference. The lower rate of quasi-periodic micro-structure at *L* band may be a result of a steeper spectrum of the micro-pulses or a lower pulse intensity modulation at higher frequencies as seen in PSR B2016+28 (Cordes et al. 1990).

4.3 Rotational period dependency of micro-structure

The dependency on pulsar rotational period of the micro-structure periodicity and width have been established in canonical pulsars for decades (Cordes 1979; Kramer et al. 2002), but only recently have they been investigated in MSPs (De et al. 2016). These relations could provide important indication of the mechanism behind micro-structure, thus constraining the angular and temporal models that explain the appearance of quasi-periodic micro-structure (e.g. Cordes et al. 1990). Using a number of measurements in canonical pulsars and two in MSPs, De et al. (2016) obtained a P–P_μ relation as $P_\mu \simeq 1.06P^{0.96}$. This predicts a micro-structure periodicity of 16.2, 15.8, and 4.2 µs for the periods of J1022+1001, J2145−0750, and J1744−1134, respectively, consistent with our measurements as summarized in Table 1. Similarly, from Kramer et al. (2002), the micro-structure width (in µs) scales with the pulsar rotational period (in ms) as $\tau_\mu \simeq 0.3P^{1.1}$. For J1022+1001, J2145−0750, and J1744−1134, this gives a micro-structure width of 6.5, 6.4, and 1.4 µs, respectively, which are qualitatively similar to the measurements in this work. Therefore, our results provide additional support for the extension of the P–P_μ and also likely the P–τ_μ relations from the canonical pulsar population to MSPs.

4.4 Possible link to fast radio bursts

Recently, a series of studies have reported the discovery of fast radio bursts (FRBs) which exhibit some stunning narrow temporal emission features, with a time-scale down to microsecond or even 100 ns level (e.g. Nimmo et al. 2021, 2022). In particular, some show quasi-periodic intensity modulation from a single burst detection (Majid et al. 2021; The CHIME/FRB Collaboration 2021; Nimmo et al. 2022), similar to the micro-structure pulses detected in radio pulsars. Indeed, The CHIME/FRB Collaboration (2021) presented an extensive discussion on the possible origin of quasi-periodic emission in three of the FRBs detected with the Canadian Hydrogen Intensity Mapping Experiment (CHIME) Telescope, where micro-structure emission mechanisms alike those invoked for radio pulsars and magnetars were considered as one of the possible explanations. Two of the FRBs reported there, i.e. FRB 20191221A and FRB 20210206A, appear to show evidence of scattering which creates an apparent overlap between each individual components. While scattering in our observations at *L* band is expected to be negligible compared with the time resolution of the data (Cordes & Lazio 2002), we could still attempt to explore if micro-structure pulses, in case of prominent scattering, can reproduce pattern similar to those seen in the CHIME bursts. In order to do so, we chose one of the pulses from PSR J1022+1001 shown in Fig. 2 (on the right), and convolved with a pulse broadening function based on the thin screen scattering model (Williamson 1972). We applied a scattering time-scale as a function of frequency as $\tau_{\rm d} \propto f^{-4.4}$, assuming a Kolmogorov spectrum, a typical spectral index of −1.8, and a $\tau_{\rm d} = 0.6$ µs at 1.4 GHz. Fig. 6 shows the simulated pulse profile starting from our observing frequency, 1.4 GHz, and spreading down to 400 MHz, the lower bound of the CHIME band. The simulation managed to reproduce the general feature of the two FRBs reported in The CHIME/FRB Collaboration (2021) (in particular FRB 20210206A in their fig. 1b), where the scattering occurs mostly at the bottom of the frequency band and creates an emission floor that lifts each individual components. It is also important to point out that the original micro-structure pulse from our observation does not have an apparent emission floor a prior to being scattered, which is consistent with what The CHIME/FRB Collaboration (2021) found for the three bursts after de-scattering them.

Though the first FRBs were found to have an apparently flat P.A. swing (Petroff et al. 2016), recent observations have started to also reveal those of more complex P.A. structures (e.g. Luo et al. 2020). Nimmo et al. (2021) showed that some of the bursts from the repeating FRB 20180916B exhibit P.A. curves with a generally flat shape but small variations within about a 10 deg range. The P.A. of FRB 20210213A also shows similar characteristics (The CHIME/FRB Collaboration 2021). These are compatible with the P.A. curves seen from the micro-structure pulses as shown in Fig. 5. If FRB emission comes from neutrons star magnetospheres, the generally flat P.A. of these FRBs may be explained by the fact that the emission is always from a very narrow pulse phase window, i.e. a small fraction of the magnetosphere where intrinsically the P.A. variation is very limited.

Assuming these FRBs with periodic structure can be associated to micro-structure emission from neutron stars, it is then indeed possible to use the P–P_μ and P–δ_μ relationships to infer the rotational period

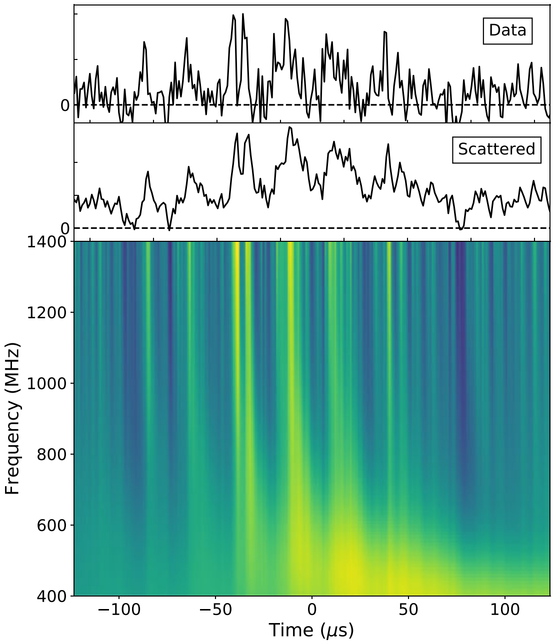

Figure 6. Simulation of scattered micro-structure pulse, using the detection from PSR J1022+1001 shown in the right-hand panel of Fig. 2. Here, we assumed a scattering time-scale of 0.6 μs at 1.4 GHz, scattering law of $\tau_{\rm d} \propto f^{-4.4}$ and a spectral index of −1.8.

of the underlying neutron star. This may provide useful input for the ongoing efforts of searching for potential periodicities in FRBs. But further evidence is needed to make such a link, so that we will expand on this idea in a separate forthcoming work.

5 CONCLUSIONS

We have detected micro-structure emission in three MSPs, PSRs J1022+1001, J2145−0750, and J1744−1134, using highly sensitive observations with LEAP at 1.4 GHz. A fraction of the pulses show quasi-periodic micro-structure features. In PSR J1022+1001 and J1744−1134 they were seen to be significantly polarized. The occurrence rate of quasi-periodic micro-structure was found to be consistent among pulses with different peak flux densities including the brightest group. Using an ACF analysis we have measured the periodicity and width of the micro-structures in these three pulsars. For PSR J1022+1001, we showed that the P.A. obtained from micro-structure pulses are from a narrow phase window and on average consistent with that of the average profile, with a small degree of variations. The results have allowed us to further examine the frequency and rotational period dependency of micro-structure properties, and thus the angular beaming and temporal modulation models that explain the appearance of micro-structure. These results have also implied a possible link to FRBs which exhibit a similar emission morphology.

ACKNOWLEDGEMENTS

We thank Laura Spitler for providing valuable comments on this manuscript. KL acknowledges the financial support by the European Research Council for the ERC Synergy Grant BlackHoleCam under contract no. 610058. JA is supported by the Stavros Niarchos Foundation (SNF) and the Hellenic Foundation for Research and Innovation (H.F.R.I.) under the 2nd Call of ‘Science and Society’ Action Always strive for excellence – ‘Theodoros Papazoglou’ (Project Number: 01431). JWM is a CITA Postdoctoral Fellow: This work was supported by Ontario Research Fund-research Excellence Program (ORF-RE) and the Natural Sciences and Engineering Research Council of Canada (NSERC) [funding reference CRD 523638-18].

This work was supported by the ERC Advanced Grant ‘LEAP’, Grant Agreement Number 227947 (PI M. Kramer). The Effelsberg 100-m telescope is operated by the Max-Planck-Institut für Radioastronomie. Pulsar research at the Jodrell Bank Centre for Astrophysics and the observations using the Lovell Telescope are supported by a consolidated grant from the STFC in the UK. The Westerbork Synthesis Radio Telescope is operated by the Netherlands Foundation for Radio Astronomy, ASTRON, with support from NWO. The Nançay Radio Observatory is operated by the Paris Observatory, associated with the French Centre National de la Recherche Scientifique. The Sardinia Radio Telescope (SRT) is funded by the Department of Universities and Research (MIUR), the Italian Space Agency (ASI), and the Autonomous Region of Sardinia (RAS), and is operated as a National Facility by the National Institute for Astrophysics (INAF). This research is a result of the Europe-wide effort to directly detect gravitational waves using pulsar timing, known as the European Pulsar Timing Array (EPTA). WZ is supported by the the National SKA Program of China (No. 2020SKA0120100) and National Natural Science Foundation of China (Nos. 12041304,11873067).

DATA AVAILABILITY

The timing data used in this article shall be shared on reasonable request to the corresponding author.

REFERENCES

Bassa C. G. et al., 2016, MNRAS, 456, 2196
Benford G., 1977, MNRAS, 179, 311
Boriakoff V., Ferguson D. C., Slater G., 1981, in Sieber W., Wielebinski R., eds, Pulsars, IAU Symposium 95. Reidel, Dordrecht, p. 199
Buschauer R., Benford G., 1980, MNRAS, 190, 945
Cairns I. H., Johnston S., Das P., 2004, MNRAS, 353, 270
Chen S. et al., 2021, MNRAS, 508, 4970
Cheng A. F., Ruderman M. A., 1980, ApJ, 235, 576
Clemens J. C., Rosen R., 2004, ApJ, 609, 340
Cordes J. M., 1979, Space Sci. Rev., 24, 567
Cordes J. M., Lazio T. J. W., 2002, preprint (astro-ph/0207156)
Cordes J. M., Weisberg J. M., Hankins T. H., 1990, AJ, 100, 1882
Craft H. D., Comella J. M., Drake F., 1968, Nature, 218, 1122
Dai S. et al., 2015, MNRAS, 449, 3223
De K., Gupta Y., Sharma P., 2016, ApJ, 833, L10
Edwards R. T., Stappers B. W., 2003, A&A, 410, 961
Hankins T. H., 1972, ApJ, 177, L11
Harding A. K., Tademaru E., 1981, ApJ, 243, 597
Hotan A. W., van Straten W., Manchester R. N., 2004, Publ. Astron. Soc. Aust., 21, 302
Jenet F., Anderson S., Kaspi V., Prince T., Unwin S., 1998, ApJ, 498, 365
Jenet F. A., Anderson S. B., Prince T. A., 2001, ApJ, 546, 394
Keith M. J., Johnston S., Levin L., Bailes M., 2011, MNRAS, 416, 346
Kramer M., Lange C., Lorimer D. R., Backer D. C., Xilouris K. M., Jessner A., Wielebinski R., 1999, ApJ, 526, 957
Kramer M., Johnston S., van Straten W., 2002, MNRAS, 334, 523
Lange C., Kramer M., Wielebinski R., Jessner A., 1998, A&A, 332, 111
Liu K. et al., 2015, MNRAS, 449, 1158
Liu K. et al., 2016, MNRAS, 463, 3239

Luo R. et al., 2020, Nature, 586, 693
Main R. A. et al., 2020, MNRAS, 499, 1468
Majid W. A. et al., 2021, ApJ, 919, L6
McKee J. W. et al., 2019, MNRAS, 483, 4784
Mitra D., Arjunwadkar M., Rankin J. M., 2015, ApJ, 806, 236
Nimmo K. et al., 2021, Nat. Astron., 5, 594
Nimmo K. et al., 2022, Nat. Astron., 6, 393
Petroff E. et al., 2016, Publ. Astron. Soc. Aust., 33, e045
Rickett B. J., Hankins T. H., Cordes J. M., 1975, ApJ, 201, 425
Sallmen S., 1998, PhD thesis, Univ. California at Berkeley
Smits R. et al., 2017, Astron. Comput., 19, 66
The CHIME/FRB Collaboration, 2021, preprint (arXiv:2107.08463)
Van Horn H. M., 1980, ApJ, 236, 899
Williamson I. P., 1972, MNRAS, 157, 55 +

This paper has been typeset from a TEX/LATEX file prepared by the author.